Identification of hyperspectral vegetation indices for Mediterranean pasture characterization.

Article · January 2009

Source: DBLP

CITATIONS
10

READS
546

7 authors, including:

Francesco Fava
University of Milan
72 PUBLICATIONS **1,661** CITATIONS
SEE PROFILE

Roberto Colombo
Università degli Studi di Milano-Bicocca
230 PUBLICATIONS **9,000** CITATIONS
SEE PROFILE

Stefano Bocchi
Università degli Studi di Milano
150 PUBLICATIONS **2,637** CITATIONS
SEE PROFILE

Michele Meroni
European Commission
152 PUBLICATIONS **7,627** CITATIONS
SEE PROFILE

International Journal of Applied Earth Observation and Geoinformation xxx (2009) xxx–xxx

Contents lists available at ScienceDirect

International Journal of Applied Earth Observation and Geoinformation

journal homepage: www.elsevier.com/locate/jag

Identification of hyperspectral vegetation indices for Mediterranean pasture characterization

F. Fava [a,b,*], R. Colombo [b], S. Bocchi [a], M. Meroni [b], M. Sitzia [c], N. Fois [c], C. Zucca [d]

[a] GeoLab, Department of Crop Science, University of Milan, Via Celoria 2, 20133 Milan, Italy
[b] Remote Sensing of Environmental Dynamics Lab., Department of Environmental Science, University of Milano-Bicocca, Piazza della Scienza 1, 20126 Milan, Italy
[c] AGRIS Sardegna, Agricultural Research Agency of Sardinia, SS 291, Km. 18,600 Sassari, Italy
[d] Desertification Research Group, University of Sassari, Via De Nicola 9, 07100 Sassari, Italy

ARTICLE INFO

Article history:
Received 28 July 2008
Accepted 19 February 2009

Keywords:
Pasture
Remote sensing
Hyperspectral indices
Biomass
Leaf area index
Nitrogen

ABSTRACT

A field experiment was carried out to assess biomass and nitrogen status in Mediterranean pastures by means of hyperspectral high resolution field radiometric data. Spectral and agronomic measurements were collected at three different pasture growth stages and in grazed–ungrazed plots distributed over an area of 14 ha. Reflectance-based vegetation indices such as simple ratio indices (SR[*i*,*j*]) and normalized difference vegetation indices (NDVI[*i*,*j*]) were calculated using all combinations of two wavelengths *i* and *j* in the spectral range 400–1000 nm. The performances of these indices in predicting green biomass (GBM, t ha^{-1}), leaf area index (LAI, m^2 m^{-2}), nitrogen content (N, kg ha^{-1}) and nitrogen concentration (N_C, %) were evaluated by linear regression analysis using the cross validated coefficient of determination (R^2_{CV}) and root mean squared error ($RMSE_{CV}$). SR involving bands in near-infrared (*i* = 770–930 nm) and in the red edge (*j* = 720–740 nm) yielded the best performance for GBM ($R^2_{CV} = 0.73$, $RMSE_{CV}$ = 2.35 t ha^{-1}), LAI ($R^2_{CV} = 0.73$, $RMSE_{CV}$ = 0.37 m^2 m^{-2}), and N ($R^2_{CV} = 0.73$, $RMSE_{CV}$ = 7.36 kg ha^{-1}). The best model performances for N_C ($R^2_{CV} = 0.54$, $RMSE_{CV}$ = 0.35%) were obtained using SR involving near-infrared bands (*i* = 775–820 nm) and longer wavelengths of the red edge (*j* = 740–770 nm). The defined indices lead to significant improvements in model predictive capability compared to the traditional SR [near-infrared, red] and NDVI [near-infrared, red] and to broad-band indices. The possibility of exploiting these results gathered at field level with high resolution spectral data (FWHM 3.5 nm) also at landscape level by means of hyperspectral airborne or satellite sensors was explored. Model performances resulted extremely sensitive to band position, suggesting the importance of using hyperspectral sensors with contiguous spectral bands.

1. Introduction

Timely assessment of forage biomass and nutritional quality is essential for evaluating pasture productivity and functioning. The quantity and quality of available forage, for example, have a major influence on the grazing distribution patterns of livestock (Bailey et al., 1996; Senft et al., 1984) and significantly affect the overall animal performance (Ball et al., 2001). Reliable information about these variables is needed by farmers and local institutions for a rational management of livestock distribution and for monitoring the state of the pasture resource at the territorial scale (Hunt et al., 2003). This could, in turn, have significant implications on land use planning and local policy making (e.g. allocation of subsidies, early measures to tackle drought crises, etc.), particularly in Mediterranean areas, where overgrazing and management practices are key factors in land degradation processes (d'Angelo et al., 2000). Traditional methods of biomass and quality parameters estimation are based on destructive sampling and laboratory chemical analyses, which are expensive and time-consuming. Thus, their potential use for monitoring purposes and for applications in large areas is limited. In this context, remote sensing techniques offer a cost-effective solution for the quantitative estimation of pasture biophysical and biochemical variables from local to regional scale.

Remote sensing data have been widely used for characterizing grassland properties (e.g. biomass, leaf area index, chlorophyll and nitrogen content) by means of field spectrometry (Asner et al., 1999; Boschetti et al., 2007; Darvishzadeh et al., 2008a,b; Gianelle and Vescovo, 2007; He et al., 2006; Mutanga and Skidmore, 2004; Mutanga et al., 2004; Starks et al., 2006a), hyperspectral airborne and satellite instruments (Beeri et al., 2007; Cho et al., 2007; Numata et al., 2008, 2007), and multispectral satellite data (Asner et al., 2004; Todd et al., 1998). Biophysical and biochemical grassland parameters are generally estimated using empirical

* Corresponding author at: GeoLab, Department of Crop Science, University of Milan, Via Celoria 2, 20133 Milan, Italy.
E-mail address: francesco.fava@unimib.it (F. Fava).

0303-2434/$ – see front matter © 2009 Elsevier B.V. All rights reserved.
doi:10.1016/j.jag.2009.02.003

relationships established using standard or multivariate regression techniques with data derived from spectral reflectance measurements. Several studies have exploited this approach, relating field data with reflectance indices (Boschetti et al., 2007; Cho and Skidmore, 2006; Gianelle and Vescovo, 2007; He et al., 2006; Mutanga and Skidmore, 2004; Todd et al., 1998; Vescovo and Gianelle, 2006), with first derivative reflectance spectra (Lamb et al., 2002; Starks et al., 2006a), and with continuum removed spectra (Beeri et al., 2007; Mutanga et al., 2004; Numata et al., 2007). These studies underline the complexity of the spectral response of mixed grasslands, especially in presence of a high fraction of non-photosynthetic vegetation (NPV) and exposed soil (Beeri et al., 2007; He et al., 2006; Boschetti et al., 2007), grazing impact (Numata et al., 2007), and canopy architecture complexity due to mixed species composition and phenology (Cho et al., 2007; Darvishzadeh et al., 2008c; Numata et al., 2008). This complexity makes the prediction of biophysical and biochemical pasture properties still challenging for the remote sensing community, especially in mixed species environments and keeping in account the temporal variability of vegetation properties during different stages of pasture growth.

The most widely used vegetation indices (VIs) are the normalized difference vegetation index (NDVI = [Ri − Rj]/[Ri + Rj]) (Rouse et al., 1974) and the simple ratio (SR = [Ri/Rj]) (Jordan, 1969), where Ri is near-infrared reflectance and Rj is red reflectance. These two-band vegetation indices are traditionally based on the contrast between low reflectance in the red, due to chlorophyll absorption, and high reflectance in the near-infrared, related to multiple scattering effects (Elvidge and Chen, 1995; Hoffer, 1978; Todd et al., 1998). During the past decades NDVI and SR have normally been calculated from satellite multispectral sensors (e.g. Landsat Thematic Mapper) characterized by few non-contiguous broad bands (>50 nm). More recently, the development of field and airborne hyperspectral sensors (e.g. Compact Airborne Spectrographic Imager-CASI, Airborne Imaging Spectrometer for Application-AISA), which provide a contiguous spectrum in several narrow bands, have opened new perspectives for defining the most informative spectral bands for use in VIs formulation. Field hyperspectral data have been employed to identify and select optimal wavebands for maximizing the sensibility of VIs to specific vegetation variables at leaf (Blackburn, 1998) and canopy level (Cho et al., 2007; Darvishzadeh et al., 2008a; Hansen and Schjoerring, 2003; Mutanga and Skidmore, 2004; Thenkabail et al., 2000). In this way, the expression of NDVI and SR have been generalized by assigning to *i* and *j* the couple of bands that allows maximizing the relationship between VIs and the variables of interest. Therefore the advantage of using hyperspectral data is the possibility to identify new wavebands for developing ad-hoc spectral indices that are well correlated to a specific variable.

The development of new VIs through field hyperspectral data is of limited applicability for landscape scale applications. Indeed, it is important to evaluate whether they are dependent on specific sensor spectral resolution and exportable to airborne and satellite instruments. For this reason several authors have compared the predictive power and stability of semi-empirical models based on narrow-band (<10 nm) VIs derived from field hyperspectral measurements to short-band (10–20 nm) and broad-band (>50 nm) VIs simulating airborne or satellite sensors response (Broge and Leblanc, 2001; Elvidge and Chen, 1995; Hansen and Schjoerring, 2003; Lee et al., 2004; Thenkabail et al., 2000). Whilst many studies focused on the comparison between indices calculated from sensors with different spectral characteristics, few studies have systematically analysed the effects of band width and position on the predictive ability of specific VIs (Zhao et al., 2005).

The objectives of this study are: (i) to analyse the variability of reflectance and vegetation properties in different pasture growth stages and appraise the impact of this variability on VI-based assessment of pasture properties, (ii) to evaluate the potential of narrow-band NDVI and SR for assessing forage quantity and quality during the whole growing season, and (iii) to ascertain the potential exportability of the defined VIs to sensors characterized by wider band widths and/or different band positions. Although recent studies underlined the advantages of using multivariate techniques, such as partial least squared regression, for hyperspectral data analysis on mixed grasslands (Cho et al., 2007; Darvishzadeh et al., 2008a), here we focused on simple narrow-band indices which may be exported to broader band sensors for landscape scale applications.

To achieve these tasks, a field experiment was planned to collect agronomic and spectral data over Mediterranean pastures characterized by mixed species composition and by high spatial and temporal variability of vegetation properties. The experiment was carried out during three different pasture growth stages and under different grazing regimes. The variables investigated were green biomass (GBM, t ha^{-1}), leaf area index (LAI, $m^2\,m^{-2}$), nitrogen content (N, kg ha^{-1}) and nitrogen concentration (N_C, %). The first two are related to the herbage mass available for feeding livestock, while nitrogen is an important parameters for pasture nutritive value definition, since it is proportional to forage crude protein content, which is a key nutrient in animal diets (Ball et al., 2001). Only few studies have estimated these variables at the same time in pastures (Beeri et al., 2007; Starks et al., 2006a,b), while their contemporary assessment is important for informing management practices (Ball et al., 2001). Appropriate VIs were defined by searching for spectral bands *i* and *j* which are best suited for estimating pasture agronomic variables using NDVI and SR. Moreover, the predictive power of semi-empirical models based on narrow-band (3.5 nm) VIs were compared with models based on short-band (~10 nm AVIRIS-like) and broad-band (>50 nm TM-like) VIs. Finally, the effect of changes in sensor band width (FWHM) and position on the accuracy of the defined semi-empirical models was analysed.

2. Materials and methods

2.1. Study area and site characteristics

The experiment was carried out during 2006 and 2007 in an experimental farm (AGRIS-Sardegna) at Foresta Burgos, located in northern Sardinia (Italy, 40°23′N, 8°54′E). The experimental field is mixed grassland that covers an area of about 14 ha. The dominant plant species in the study site are annual and perennial grasses of the species *Hordeum murinum* L., *Lolium rigidum* Gaudin, *Avena sterilis* L., *Avena barbata* Pott ex Link, *Bromus hordeaceus* L., *Poa pratensis* L. and *Poa annua*. Beside, plants of the families Leguminosae, Compositae, Ranuncolaceae, Borraginaceae, Plantaginaceae and Geraniaceae are represented, forming a highly diverse and heterogeneous canopy. The site was historically managed as an extensive pasture, with low to medium grazing pressure levels (0.5–0.7 cattle unit ha^{-1}). The soil is a Haplic cambisol (FAO/ISRIC/ISSS, 1998), typical of the region, with an average depth of 50 cm, loam texture and a topsoil characterized by "rhizomull" (Green et al., 1993). The climate of the area is Mediterranean. Average annual precipitation is 740 mm with precipitation maxima in autumn (September to December, 330 mm), secondary maxima in spring (March to June, 245 mm) and minima in July and August (40 mm). Rainfall intensity and distribution during the experiment was close to the average with 290 mm rainfall in autumn and 294 mm in spring. The growing

Please cite this article in press as: Fava, F., et al., Identification of hyperspectral vegetation indices for Mediterranean pasture characterization. Int. J. Appl. Earth Observ. Geoinform. (2009), doi:10.1016/j.jag.2009.02.003

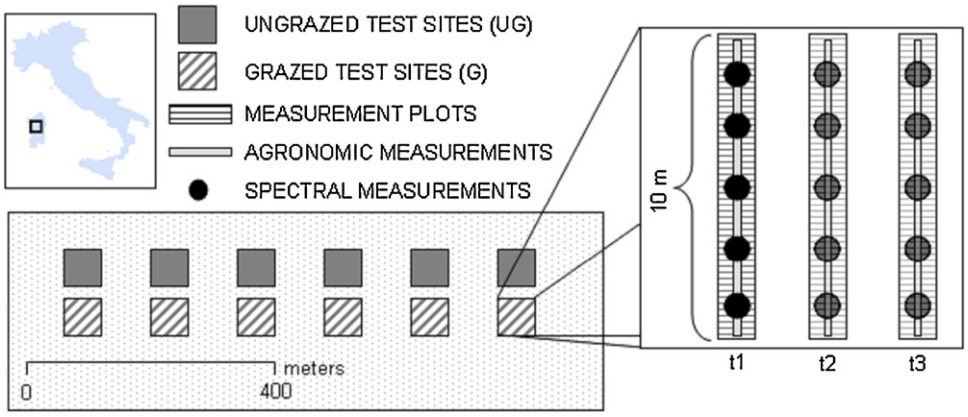

Fig. 1. Schematic representation of test sites in the experimental field. Spectral and agronomic measurements were performed in one randomly located plot in each test site in late autumn 2006 (t1), early spring 2007 (t2) and late spring 2007 (t3).

season lasts from October to June with a short break, due to low temperature, in late December and January.

2.2. Sampling scheme and data collection

The experimental setup was planned to collect a data set representative of the spatial and temporal variability of grassland properties under natural conditions. Differences in grazing pressure were also taken into account. Data were collected during three field campaigns conducted in different periods of pasture growth: late autumn 2006 (Day of the year, DOY 346-2006), early spring 2007 (DOY 107-2007) and late spring 2007 (DOY 141-2007). In the experimental field twelve homogeneous test sites of 10 m × 10 m were established: six were located in exclusion fences to avoid grazing (ungrazed sites, UG), the other six were placed in grazed areas (grazed sites, G) (Fig. 1). Test sites were located using a stratified random sampling scheme, where strata were defined accordingly to transitions in vegetation communities and grazing pressure, as indicated by farm managers. During each experimental campaign, one plot (a linear transect 10 m long) was randomly located within each test site, avoiding the same area of previous field campaigns (Fig. 1). Spectral reflectance and agronomic measurements were acquired along each plot, following standard agronomic sampling strategies used on pastures (Boschetti et al., 2007; Corrall and Fenlon, 1978; Gianelle and Vescovo, 2007). Since one exclusion fence was damaged during the last campaign, 35 plots in all were monitored. In the grazed area grazing pressure was kept constant at 0.5 cattle unit ha^{-1} in autumn and early spring. In late spring grazing was suspended in half of the grazed test sites for hay production, while it was raised at 1 cattle unit ha^{-1} in the remaining test sites, according to the management practices traditionally employed in the area.

2.2.1. Agronomic measurements

Biomass was clipped within each plot in one 10 cm per 10 m strip (1 m^2) (Fig. 1). Total biomass was weighted after cutting and sub-samples were used for dry weight determination, after drying at 60 °C till constant weight. Green biomass (t ha^{-1}) and non-photosynthetic vegetation (NPV, t ha^{-1}) were manually separated and subsequently weighted. Leaf area index (m^2 m^{-2}) of the green biomass was calculated using a Leaf Area Scanner (Li-cor 3100 C). Nitrogen concentration (N_C, %) and nitrogen content (N, kg ha^{-1}) of total biomass were determined by near-infrared reflectance (NIR) spectroscopy laboratory measurement. In order to test the effects of growing stage and grazing on the monitored agronomic variables one way analysis of variance (ANOVA) was performed.

2.2.2. Radiometric measurements

Reflectance data were collected by means of an ASD Fieldspec HandHeld spectroradiometer. This instrument acquires spectra in the visible and near-infrared region (325–1075 nm) with a Full Width Half Maximum (FWHM) of 3.5 nm and a spectral resolution of 1 nm. A cosine diffusor foreoptic was used and reflectance was calculated as the ratio between vegetation irradiance (sensor pointing nadir) and sky irradiance (sensor pointing zenith). This measurement configuration offers interesting advantages from an operational point of view because it allows fast measurements without the need for a white reference calibrated panel. To minimize operator influence the radiometer was placed on a tripod with a rotating horizontal arm. The foreoptic was positioned 70 cm above canopy height. Considering that the radiance upwelling from the target is "weighted" by cosine law in the measured upwelling irradiance, 90% of the signal came from a circular area having a radius of 1.92 m. Spectra were collected in clear sky conditions around solar noon every 2 m along each plot (5 measurement spots per plot) (Fig. 1). Each spectrum was calculated as the average of 15 readings. Finally, for each spectral measurement a hemispherical digital photograph was acquired using a Nikon Coolpix 8400 digital camera with a fish-eye lens (Nikon FE-E8 8 mm). Photographs were acquired downward keeping the camera levelled. Images were then analysed semi-automatically by Can Eye software version 5.0[1] to compute the soil cover fraction (S_C).

2.3. Spectral data analysis

2.3.1. Spectral indices identification

The analysis of the relationships between reflectance and agronomic variables focused on GBM, LAI, N and N_C retrieval, while S_C and NPV were reported only as ancillary information for better interpreting the results. A correlation analysis between spectral reflectance and the investigated variables was first performed. Subsequently, NDVI [*i*,*j*] and SR [*i*,*j*] were calculated using all possible two-band *i* and *j* combinations between 400 and 1000 nm (180600 combinations) with the aim of extracting the most relevant information available from hyperspectral data. This procedure allowed selection of optimal bands to be used in the calculation of the index with the criteria of maximizing the relationships with the variables investigated. An Ordinary Least Square (OLS) linear regression analysis was performed among all indices (independent variable) and the agronomic variables investigated (dependent variables) to identify which spectral bands were more responsive to pasture characteristics. The

[1] http://www.avignon.inra.fr/can_eye/.

Please cite this article in press as: Fava, F., et al., Identification of hyperspectral vegetation indices for Mediterranean pasture characterization. Int. J. Appl. Earth Observ. Geoinform. (2009), doi:10.1016/j.jag.2009.02.003

Table 1
Mean (±S.D.) values of green biomass (GBM), leaf area index (LAI), nitrogen content (N), nitrogen concentration (N_C), non-photosynthetic vegetation (NPV), and soil cover (S_C) measured during each field campaign in ungrazed (UG) and grazed (G) areas. Phenology of dominant grasses is also reported. NPV, S_C and phenology were not analysed with respect to spectral data.

Variable	Autumn 2006		Early spring 2007		Late spring 2007	
	UG	G	UG	G	UG	G
GBM (t ha^{-1})	3.95 (0.68)	2.42 (0.77)	5.67 (1.97)	1.59 (0.63)	13.37 (3.03)	3.19 (1.16)
LAI (m^2 m^{-2})	1.03 (0.18)	0.65 (0.18)	1.19 (0.38)	0.40 (0.16)	2.19 (0.61)	0.61 (0.26)
N (kg ha^{-1})	26.32 (4.36)	17.33 (4.37)	28.13 (9.65)	9.42 (3.44)	44.65 (12.29)	13.94 (3.72)
N_C (%)	2.16 (0.25)	2.00 (0.14)	2.42 (0.30)	2.74 (0.28)	1.24 (0.23)	1.87 (0.35)
NPV (t ha^{-1})	1.82 (0.71)	1.27 (0.69)	0.39 (0.26)	0.10 (0.08)	0.10 (0.17)	0.00
S_C (%)	13.75 (7.49)	12.53 (5.89)	4.88 (3.14)	11.06 (7.84)	0.00	5.97 (4.95)
Phenology	Tillering		Stem elongation		Flowering-ripening	

coefficient of determinations (R^2) resulting from the regression analysis were plotted on a contour plot to evaluate R^2 characteristic patterns. Homogeneous areas of high R^2 value (between 90% and 100% of the overall maximum R^2) were identified and defined as "hotspots" according to Hansen and Schjoerring (2003). This threshold was set to facilitate interpretation of the contour plot and to drive the selection of indices well related to the variables investigated. The two-band vegetation index with the highest R^2 value in each hotspot was selected and included in further analyses. Besides linear regression, an exponential fit was tested in order to evaluate potential saturation effects on the selected indices. Finally, predictive performances of the overall best models for GBM, LAI, N, and N_C were calculated with a leave-one-out (LOO) cross-validation and expressed as cross-validated coefficient of determination (R^2_{CV}) and cross-validated root mean square error ($RMSE_{CV}$).

2.3.2. Sensor band width and position analysis

Selected ASD Fieldspec narrow-band indices for each hotspot were compared with short-band and broad-band indices based on simulated spectra of airborne hypespectral sensors and satellite multispectral sensors. In this study we decided to simulate airborne AVIRIS (Airborne Visible/Infrared Imaging Spectrometer) short-band spectra and satellite TM (Landsat Thematic Mapper) broad-band spectra. These sensors are representatives of broad sensor classes: the ASD Fieldspec is representative of hyperspectral field spectrometers and latest generation hyperspectral airborne sensors (e.g. CASI, AISA); AVIRIS is representative of first generation hyperspectral airborne sensors characterized by FWHM between 8 and 20 nm (e.g. DAIS, MIVIS). Finally, the TM sensor is used as a reference of broad-band satellite instruments (e.g. ASTER, SPOT, Quickbird). Spectral resampling from ASD Fieldspec channels to simulated sensors were performed using the spectral resampling routine available on ENVI 4.3 software (Research Systems, Inc.). Sensor-specific spectral response functions were set for TM channels, while Gaussian response functions were assumed for AVIRIS.

Afterwards, the effect of band width broadening and of sensor spectral shift on the relationship between selected VIs and agronomic variables was considered in detail. The effect of band width was studied by degrading the FWHM from 3.5 nm to 50 nm. The influence of sensor band position was evaluated by simulating a band centre shift for each of the bands included in the index one at once. Results were expressed in terms of percent variation in model estimation accuracy (i.e. R^2).

3. Results

3.1. Effect of growing stage and grazing on agronomic variables

Summary statistics of pasture agronomic variables for the three measurement campaigns and in grazed (G) and ungrazed (UG) plots are given in Table 1. The seasonal dynamics of investigated variables were linked to the phenological development of dominant grasses. GBM, LAI and N remained relatively constant on average between autumn and early spring, until stem elongation started. Subsequently, they increased rapidly. NPV had an opposite trend, with high values in autumn, up to 40% of the total biomass, and very low values in the other two campaigns. S_C decreased constantly throughout the season. N_C varied differently from N, with a peak in early spring and a minimum value in late spring, when dominant grasses were between flowering and ripening phase. Ungrazed plots had generally lower GBM, LAI and N than grazed plots. The NPV value resulted lower too, but with heterogeneity within the plots as indicated by high standard deviations. S_C and N_C were slightly higher in grazed areas than in ungrazed areas.

Table 2
Correlation matrix between investigated pasture variables.

	GBM	LAI	N	N_C	NPV	S_C
GBM (t ha^{-1})	1.00					
LAI (m^2 m^{-2})	0.95*	1.00				
N (kg ha^{-1})	0.92*	0.96*	1.00			
N_C (%)	−0.66*	−0.60*	−0.51	1.00		
NPV(t ha^{-1})	−0.26	−0.12	0.00	0.10	1.00	
S_C (%)	−0.60*	−0.56*	−0.51	0.31	0.47	1.00

* Correlation coefficient significant at $p < 0.001$.

According to the ANOVA analysis, both growth stage and grazing treatment had a significant effect on GBM, LAI, and N ($p < 0.001$), while only growth stage had a significant effect on S_C and NPV ($p < 0.001$). N_C changed mainly with growth stage ($p < 0.001$), but also grazing had a minor impact ($p < 0.01$).

Table 2 lists the linear correlation coefficients between the measured agronomic variables. GBM, LAI and N were highly and positively inter-correlated. N_C had a weaker negative correlation with GBM and LAI and was not significantly correlated with N. NPV was not significantly correlated with any other agronomic variable, while S_C showed a negative correlation with GBM and LAI.

3.2. Correlation between reflectance and agronomic variables

Reflectance decreased in the whole spectrum as the season progressed, with a major reduction between the autumn and early spring campaigns (Fig. 2a). Ungrazed and grazed plots presented smaller differences (Fig. 2b). The presence of more GBM in the ungrazed plots with respect to the grazed ones is not clearly detected by the average reflectance spectra depicted in Fig. 2b.

The correlation between spectral reflectance in the 600 bands and each pasture variable investigated showed a marked seasonal variability (Fig. 3). GBM, LAI and N were always negatively correlated with visible (VIS) reflectance, with maxima correlations in early spring in the red (600–700 nm) and blue (400–500 nm)

Please cite this article in press as: Fava, F., et al., Identification of hyperspectral vegetation indices for Mediterranean pasture characterization. Int. J. Appl. Earth Observ. Geoinform. (2009), doi:10.1016/j.jag.2009.02.003

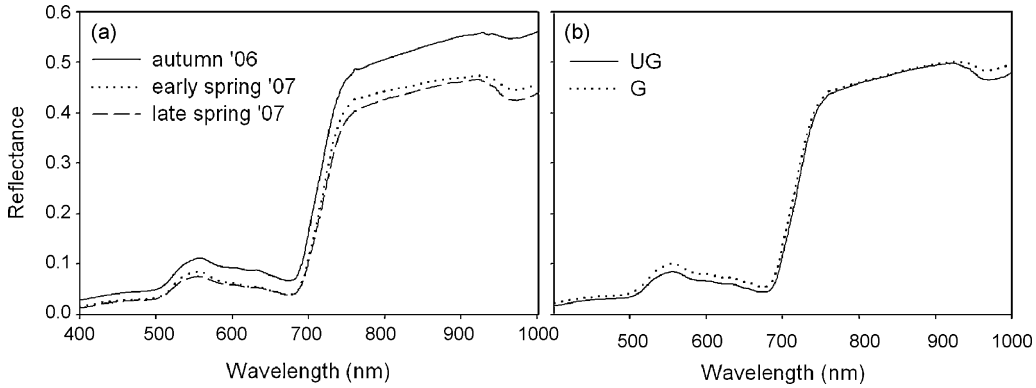

Fig. 2. Average reflectance spectrum measured in: (a) the different experimental campaigns (b) in grazed (G) and ungrazed (UG) plots.

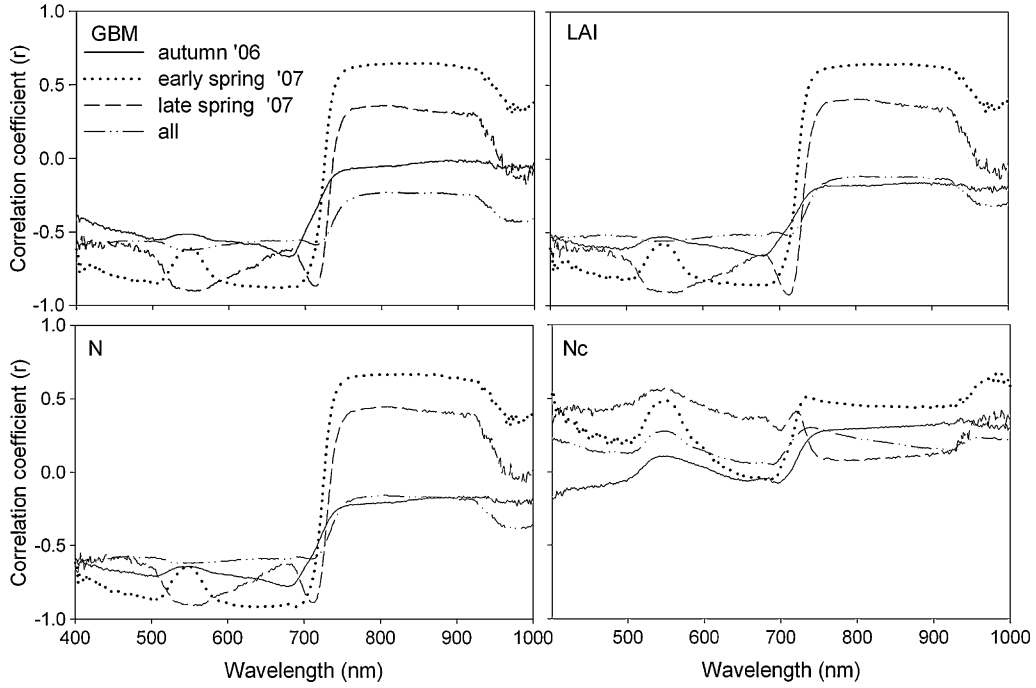

Fig. 3. Correlogram between spectral reflectance in the 400–1000 nm range and GBM, LAI, N, and N_C obtained in autumn 2006 (n = 12), early spring 2007 (n = 12), late spring 2007 (n = 11), and in the whole season (n = 35).

regions and generally lower correlations in autumn. The near-infrared reflectance (NIR) was positively correlated with GBM, LAI and N only in autumn and early spring, while almost absent correlations were observed in late spring. The correlation curve for N_C had a different shape, characterized by weak positive correlations in the whole spectrum, with maxima in the NIR during early spring and in the green bands (520–580 nm) during late spring. Considering the pooled data set, the NIR reflectance was weakly correlated with GBM, LAI, and N, while stronger negative correlations were observed with visible reflectance (VIS). N_C was poorly correlated with reflectance in the whole spectral range.

3.3. Hotspot identification and optimal index selection

The contour plot in Fig. 4 represents the coefficients of determination resulting from the regression analysis of the investigated variables against SR obtained combining all possible pairs of wavelengths i and j in the range 400–1000 nm, using the pooled data set. All possible NDVI were also calculated with comparable patterns and slightly lower R^2 values (data not shown).

Variables expressed per unit area, namely GBM, LAI and N, had similar patterns (Fig. 4a–c): a total of three hotspots were identified; the first hotspot (HS1) was located where NIR bands (i = 770–930 nm) coincided with shorter wavelengths of the red edge (j = 720–740 nm). This area presented the overall maxima R^2 values. The second hotspot (HS2), found only for GBM and N, was centred on ratio between NIR bands (i = 800–940 nm) and green bands (j = 535–565 nm). The third hotspot (HS3) was observed only for GBM in the region where water absorption bands (i = 960–970 nm) coincided with NIR shoulder bands (j = 915–930 nm). Fig. 4d shows the pattern found for N_C. This pattern is different with generally lower R^2 values. The highest R^2 values (HS4) were provided by SR employing bands in the NIR (i = 775–820 nm) and in the longer wavelength of the red edge (j = 740–770 nm).

The percentage of narrow bands included in the hotspots for each variable is shown in Fig. 5. Red edge bands were the most frequent with maximum percentages between 700 and 750 nm for GBM, LAI and N and between 750 and 800 nm for N_C. High frequencies for GBM, LAI and N were also located in the NIR plateau. In the green region relevant frequencies were evident for N and GBM.

Please cite this article in press as: Fava, F., et al., Identification of hyperspectral vegetation indices for Mediterranean pasture characterization. Int. J. Appl. Earth Observ. Geoinform. (2009), doi:10.1016/j.jag.2009.02.003

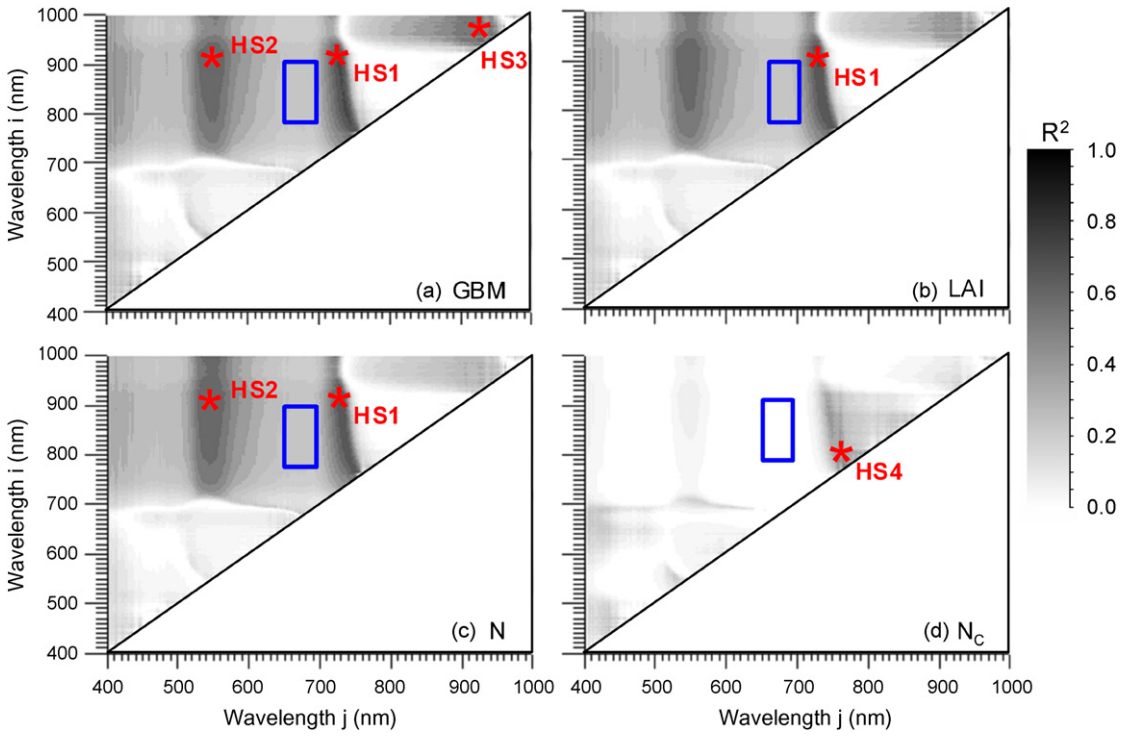

Fig. 4. Contour plot representing the coefficient of determination (R^2) of the OLS regression between SR obtained with all possible two-band *i* and *j* combinations in the 400–1000 spectral range and GBM, LAI, N, N_C (n = 35). Hotspots centre (HS) is shown in red stars. The spectral region included in the standard SR is reported in the blue box for comparison. (For interpretation of the references to color in this figure legend, the reader is referred to the web version of the article.)

Linear regression models between the index showing the overall best performance and the investigated variables are reported in Fig. 6. Models with standard SR defined with NIR and red bands are included for comparison. Exponential models were also tested with no significant improvement for any of the investigated indices (data not shown). Similar R^2_{CV} values (0.73) were obtained for GBM, LAI and N predictive models, while $RMSE_{CV}$ were 2.35 t ha^{-1}, 0.37 m^2 m^{-2} and 7.36 kg ha^{-1}, respectively. For N_C R^2_{CV} was 0.54, while $RMSE_{CV}$ was 0.35%.

The relationship between standard SR and the investigated variables was different in the three measurements periods, which are clearly separated in the scatter plots (Fig. 6b, d, f, h). The wider offset was evidenced in the late spring campaign, especially in plots where dominant grasses were in the ripening phase. These plots exhibited similar standard SR values for higher GBM and lower N_C than the previous measurements periods. On the contrary, the selected optimal indices did not present offsets between measurement campaigns and showed a linear response during the whole season (Fig. 6a, c, e, g).

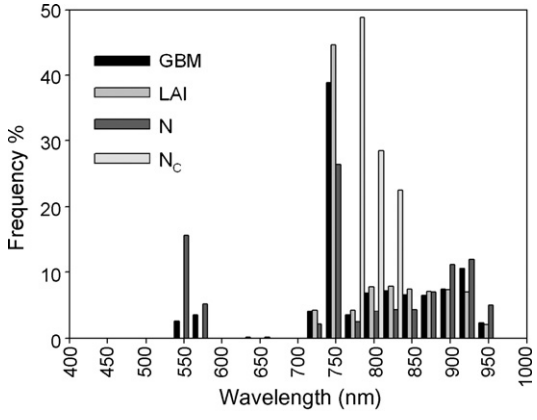

Fig. 5. Occurrence of bands in the hotspots individuated for GBM, LAI, N, N_C. The histogram bind width is 25 nm.

3.4. Effect of sensor band width and position on model accuracy

Results of the linear regression analysis between agronomic variables and the best SR defined in each hotspot, simulated AVIRIS short-band indices, and broad-band TM indices are reported in Table 3. Models based on narrow-band indices and short-band indices showed similar performance for GBM, LAI and N estimation. For N_C a decrease in R^2 of approximately 8% was observed in the model based on short-band index. This was likely related to the narrow hotspot region in which the index was selected. TM-like broad-band indices always had a poorer performance than hyperspectral ones. The best index for GBM, LAI and N estimation was SR calculated with NIR and green bands (R^2 = 0.59), while no index was significantly related to N_C.

To better understand the effect of FWHM and band position on the overall best model performance, an increase in FWHM and a shift in band position were simulated and a regression analysis repeated. The contour plots in Fig. 7 illustrate the percent variation of R^2 as a function of band shift and FWHM for each of the best models previously defined. For bands located in the red edge region a subtle band shift of less than 5 nm produced a reduction of 5% in the correlation (Fig. 7b, d, f, h). The same steep reduction of R^2 was observed shifting the band located at 920 nm towards longer wavelengths (Fig. 7a). On the contrary, a R^2 decrease of 5% resulted for a shift in NIR bands of 20 nm or larger (Fig. 7c, e), likely due to the stability of the NIR plateau region. The poor vertical gradient observed in the contour plots indicates that the selected spectral indices were only slightly affected by a variation in FWHM. In this case, an increase in FWHM between 7 and 35 nm produced a decrease in R^2 of less than 5%.

Please cite this article in press as: Fava, F., et al., Identification of hyperspectral vegetation indices for Mediterranean pasture characterization. Int. J. Appl. Earth Observ. Geoinform. (2009), doi:10.1016/j.jag.2009.02.003

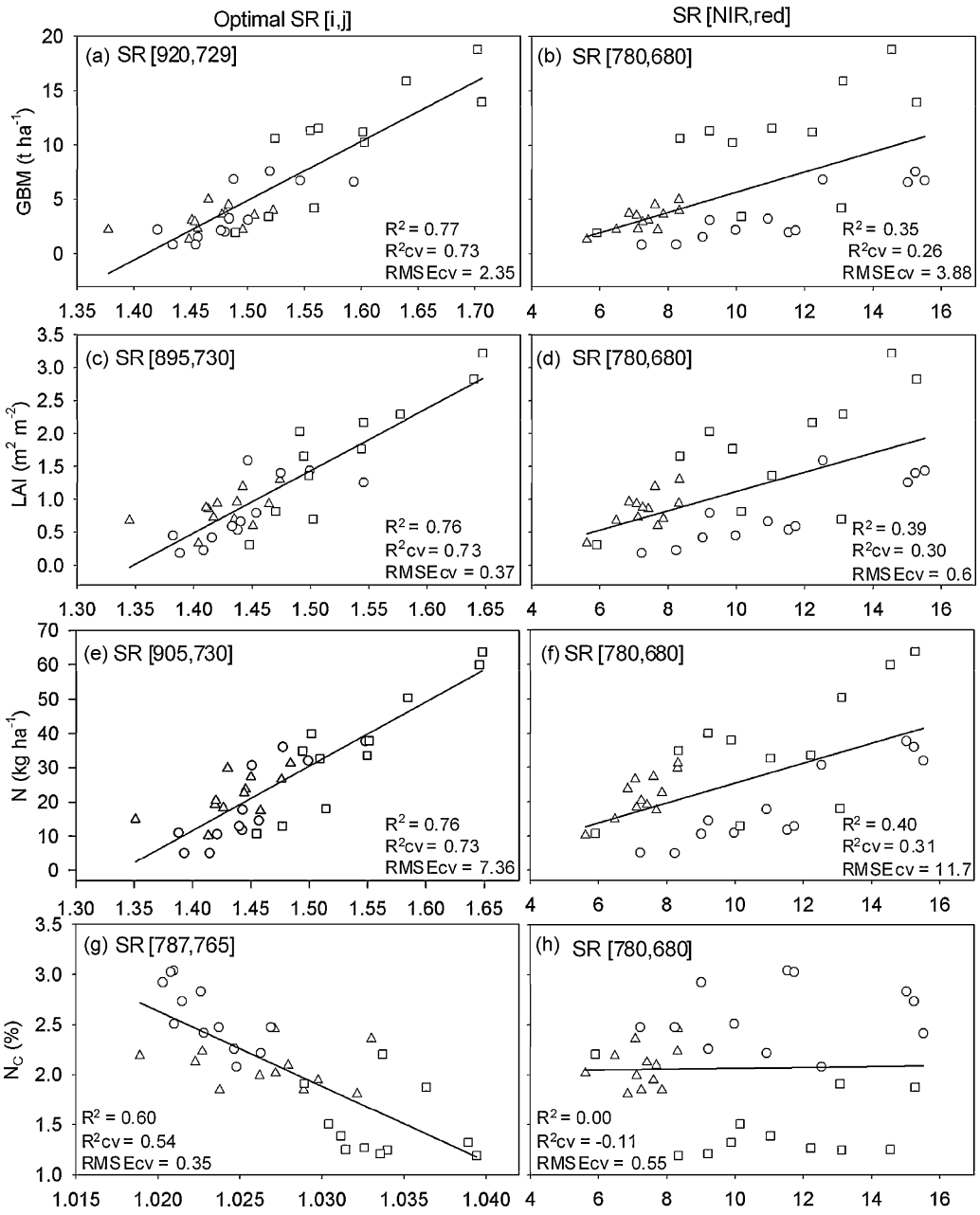

Fig. 6. Linear regression models between optimal SR (left side), standard SR [NIR, red] (right side) and GBM (a, b), LAI (c, d), N (e, f), N_C. (g, h) ($n = 35$). For each model R^2, R^2_{CV}, and $RMSE_{CV}$ are reported. Symbols represent measurements campaigns: (Δ) autumn 2006, (○) early spring 2007 (□) late spring 2007.

4. Discussion

The analysis of the spatial and temporal variability of Mediterranean pastures properties showed that primarily growing stage and to a lesser extent grazing influenced pasture biomass and nitrogen status (Table 1). Hence, both factors should be considered to build a robust data set for semi-empirical model development. GBM, LAI and N, all variables expressed per unit ground area, were highly inter-correlated ($r > 0.9$, Table 2) and this made their independent prediction difficult. The inter-correlation between N_C and the other variables was lower (<0.7, Table 2), making more feasible to test the ability of hyperspectral data for the independent assessment of forage quantity and quality parameters.

The correlation analysis between spectral reflectance and the investigated variables illustrates the complexity of the spectral response of Mediterranean grasslands characterized by mixed species composition. GBM, LAI, N and N_C exhibited a strong seasonal variability of the correlation pattern (Fig. 3), that was likely related to the contrasting effect on reflectance of several factors acting in different periods of vegetation growth. The lowest correlations in the whole spectrum were observed during the autumn campaign, characterized by a high fraction of NPV and average S_C of about 15%. As suggested by several authors, both NPV and S_C may have strong effects on reflectance (Asner, 1998; Boschetti et al., 2007; He et al., 2006; Van Leeuwen and Huete, 1996; Rundquist, 2002) and may reduce the strength of correlation with the investigated variables. During early and late spring campaigns, the correlation pattern did not differ from those generally reported in literature for grasslands (e.g. Gianelle and Guastella, 2007; Starks et al., 2006a), although correlation values were lower in late than in early spring. This variability was reflected on the relationship defined using the pooled data set: VIS

Please cite this article in press as: Fava, F., et al., Identification of hyperspectral vegetation indices for Mediterranean pasture characterization. Int. J. Appl. Earth Observ. Geoinform. (2009), doi:10.1016/j.jag.2009.02.003

Table 3
Coefficient of determination (R^2) of OLS regression models between selected SR, short-band AVIRIS-like simulated SR, broad-band TM-like simulated SR and GBM, LAI, N, N_C ($n = 35$). R^2 values over 0.6 are highlighted.

Index type	Band center [i,j] (nm)	Band width (FWHM) (nm)	Coefficient of determination (R^2)			
			GBM	LAI	N	N_C
Narrow-band SR (3.5 nm)	[920,729]	3.5	**0.77**	-	–	–
	[923,553]	3.5	**0.70**	–	–	–
	[964,923]	3.5	**0.69**	–	–	–
	[895,730]	3.5	–	**0.76**	–	–
	[905,730]	3.5	–	–	**0.76**	–
	[926.544]	3.5	–	–	**0.70**	–
	[787,765]	3.5	–	–	–	**0.60**
Short-band (AVIRIS) SR (10 nm)	[923,731]	8.5	**0.75**	–	–	–
	[923,557]	8.5	**0.69**	–	–	–
	[961,923]	8.5	**0.65**	–	–	–
	[894,731]	8.5	–	**0.75**	–	–
	[904,731]	8.5	–	–	**0.75**	–
	[923,547]	8.5	–	–	**0.69**	–
	[787,765]	8.5	–	–	–	0.55
Broad-band (TM) SR (>50 nm)	TM1 [4-3]	140-60	0.39	0.39	0.40	0.00
	TM2 [4-2]	140-60	0.59	0.58	0.58	0.04
	TM3 [4-1]	140-70	0.44	0.45	0.44	0.01
	TM4 [2-3]	60	0.09	0.09	0.08	0.09
	TM5 [1-2]	70-60	0.33	0.28	0.23	0.02
	TM6 [1-31	70-60	0.07	0.06	0.07	0.12

reflectance decreased with increasing GBM, LAI and N, as expected, due to increased light absorption by photosynthetic pigments (Hinzman et al., 1986). On the contrary, NIR response was not directly related to GBM, LAI and N, as already reported in other studies involving multi-temporal data sets (Gianelle and Vescovo, 2007). N_C resulted poorly related to reflectance in the whole spectrum, consistently with Hansen and Schjoerring (2003).

The definition of all the possible two-band combinations for SR and NDVI calculation allowed selecting optimal bands for GBM, LAI, N and N_C estimation, considering the pooled data set. SR performed always better than NDVI and the hotspots evidenced by the two indices were the same. For these reason further analyses focused on SR. Different hotspots for GBM, LAI and N estimation were evidenced (Fig. 4), all reported as recommended areas for hyperspectral studies on crops (Thenkabail et al., 2000). Results were also consistent with those of Cho et al. (2007) and Darvishzadeh et al. (2008a) for LAI estimation in heterogeneous grasslands and of Hansen and Schjoerring (2003) for GBM, LAI and N estimation in wheat crops. The hotspot observed for GBM in the moisture-sensitive bands around 970 nm was also indicated in previous studies, which reported this area as strongly influenced by canopy dry matter content as well as water content (Bowyer and Danson, 2004). In general, the use of red edge bands (700–730 nm) and green bands (535–565 nm) instead of red absorption peak bands (660–690 nm) as the denominator in index calculation allowed enhancement of the ability of the index to fit GBM, LAI and N (Figs. 4 and 5). The main hotspot for N_C included bands in the longer wavelengths of the red edge (740–770 nm) and in the NIR (Fig. 4). High correlations were observed also in the chlorophyll $a + b$ absorption features in the VIS region (Hansen and Schjoerring, 2003). Maximum R^2 values were lower than area-related variables, consistently with other studies (Feng et al., 2008; Gianelle and Guastella, 2007; Hansen and Schjoerring, 2003). This is not surprising since N_C estimation is essentially based on its direct relationship with chlorophyll concentration (Everitt et al., 1985; Lamb et al., 2002), which is difficult to estimate by simple ratio indices for LAI values below 3 because of the influence of canopy architecture (e.g. LAI) that masks chlorophyll effects (Daughtry et al., 2000; Haboudane et al., 2002; Zarco-Tejada et al., 2001).

The accuracy obtained by the best predictive models defined for GBM, LAI, N and N_C (Fig. 6) was comparable with previous results reported for mixed grasslands (Cho et al., 2007; Darvishzadeh et al., 2008a; Gianelle and Guastella, 2007; Starks et al., 2006a). The selection of optimal SR bands allowed an improvement in the relationships for all the variables investigated compared to standard SR. These improvements were more significant for N_C, with an increase in R^2_{CV} of 0.54 compared to standard SR. Likewise correlations with reflectance, the relationship between standard SR and all the investigated variables resulted strongly affected by factors related to vegetation growth stage, as clearly depicted by the samples distribution in the scatter plots (Fig. 6b, d, f, h). On the contrary, the selected SR were able to normalize the effect of these factors. The low sensitivity of standard SR to LAI and biomass have been generally associated with saturation problems (Danson and Plummer, 1995; Mutanga and Skidmore, 2004). In this study LAI values were generally lower than 2.5 $m^2\,m^{-2}$ and saturation effects were not evident (Fig. 6b, d), while the wider offset was observed in plots with dominant grasses in the ripening phenological phase, as already reported by Inoue et al. (2008). For this reason we suggest that phenological stage should be carefully considered when developing statistical models for mixed grassland properties estimation.

The potential of exploiting the models gathered at field level at the landscape level was evaluated by simulating from our data set AVIRIS-like short-band (10–20 nm) spectra and TM-like broad-band (>50 nm) spectra. Narrow-band SR based on field data or short-band SR based on AVIRIS data exhibited similar performances (Table 3). Both of them had better performances than broad-band TM based indices (R^2 increase from 0.18 to 0.60) in estimating all the agronomic variables monitored, especially for N_C, in agreement with recent findings of Gianelle and Vescovo (2007), Hansen and Schjoerring (2003) and Vescovo and Gianelle (2006). Moreover, our results showed that even a small shift in band position (5 nm) would produce a reduction in the R^2 value from 0.02 to 0.07, especially for models based on VIs involving bands in the red edge (Fig. 7). On the contrary, FWHMs exerted a minor role in spectral index performances, showing that the semi-empirical models defined in this study would be exportable to narrow-band (CASI, AISA) or short-band (e.g. AVIRIS, DAIS,

Please cite this article in press as: Fava, F., et al., Identification of hyperspectral vegetation indices for Mediterranean pasture characterization. Int. J. Appl. Earth Observ. Geoinform. (2009), doi:10.1016/j.jag.2009.02.003

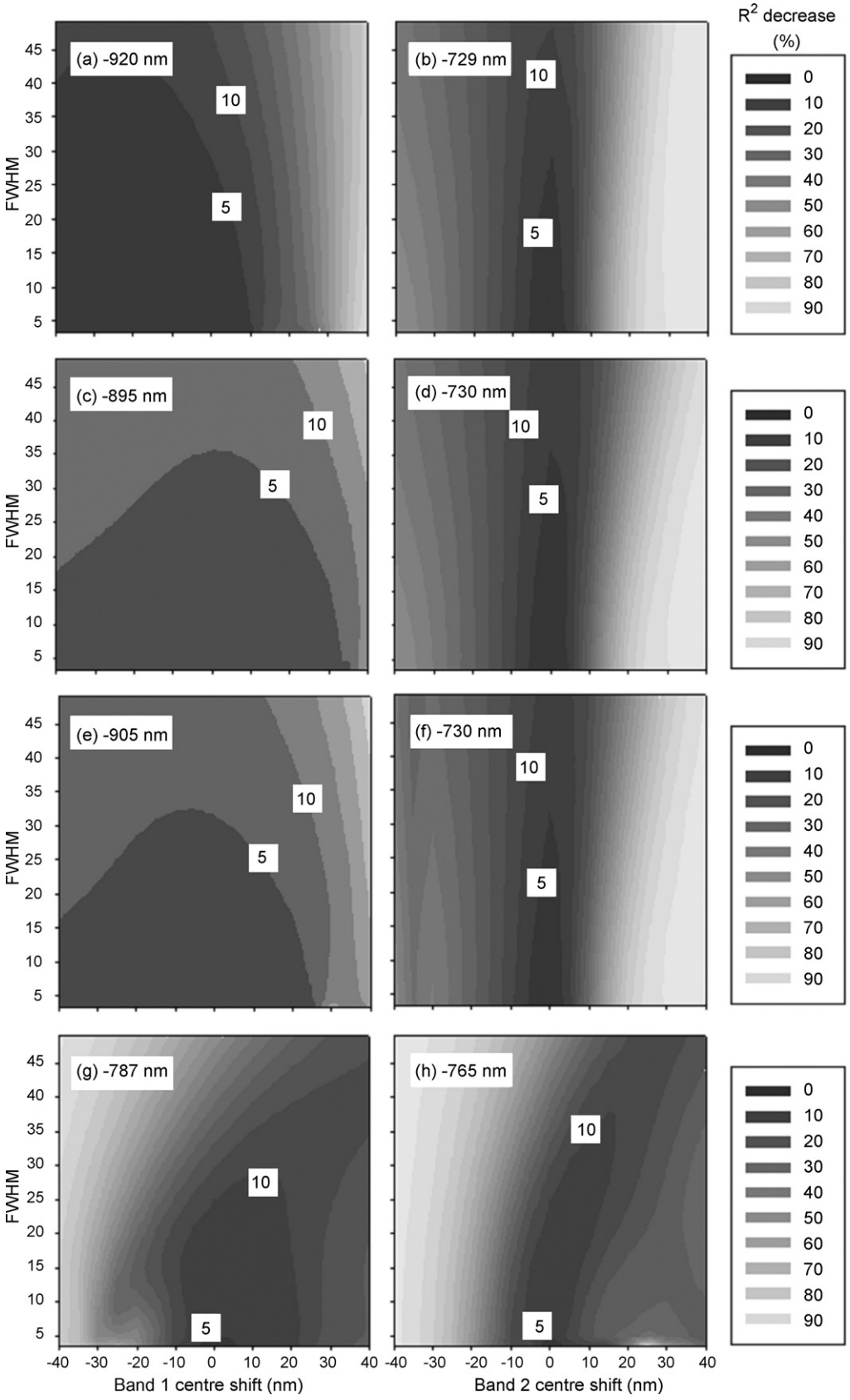

Fig. 7. Percent decrease of the coefficient of determination (R^2) of best linear regression models defined for GBM (a, b), LAI (c, d), N (e, f) and N_C (g, h) as a function of SR band 1 shift (left side), SR band 2 shift (right side) and FHWM.

Please cite this article in press as: Fava, F., et al., Identification of hyperspectral vegetation indices for Mediterranean pasture characterization. Int. J. Appl. Earth Observ. Geoinform. (2009), doi:10.1016/j.jag.2009.02.003

HYPERION) airborne or satellite sensors with minimal loss of accuracy. Indeed, the main limitations connected with broad-band indices for assessing pasture biophysical properties were related to the reduced number of bands that did not allow identification of the best spectral region for variable estimation, more than to the wide FWHM, as already reported by Broge and Leblanc (2001).

5. Conclusions

In this study we analysed the spectral response of heterogeneous Mediterranean pastures by means of hyperspectral remote sensing data acquired in the field. The data set was built in order to keep in account both the spatial and temporal variability of pasture properties, explicitly considering the effects of grazing and growth stage on reflectance data. Narrow-band NDVI and SR were used for predicting GBM, LAI, N, and N_C by means of ordinary regression models, evaluated by R^2_{CV} and $RMSE_{CV}$ through cross-validation. Moreover, the potential of exploiting the regression models gathered at field level at the landscape level was evaluated by simulating from our data set AVIRIS-like short-band (10–20 nm) spectra and TM-like broad-band (>50 nm) spectra and through a systematic analysis of the effect of sensor band width (FWHM) and position on model accuracy.

The main conclusions of this study can be summarized as follows:

(i) The contrasting effects of factors acting in different periods of pasture growth, such as S_C, NPV, and vegetation phenology induced a strong seasonal variability in the correlation between reflectance and GBM, LAI, N and N_C. This was reflected also in the relationship with standard SR, which changed along the season, particularly during the ripening phenological stage of dominant grasses.

(ii) Narrow-band SR performed always better than narrow-band NDVI for GBM, LAI, N, and N_C estimation.

(iii) Narrow-band SR involving bands located in the NIR (i = 770–930 nm) and in the red edge (j = 720–740 nm) resulted the best suited for GBM ($R^2_{CV} = 0.73$, $RMSE_{CV}$ = 2.35 t ha^{-1}), LAI ($R^2_{CV} = 0.73$, $RMSE_{CV}$ = 0.37 m^2 m^{-2}), and N ($R^2_{CV} = 0.73$, $RMSE_{CV}$ = 7.36 kg ha^{-1}) prediction. For N_C, best model performances were achieved using NIR bands (i = 775–820 nm) and longer wavelengths of the red edge (j = 740–770 nm) ($R^2_{CV} = 0.54$, $RMSE_{CV}$ = 0.35%). These indices were not affected by the above-mentioned effects related to pasture growth stage.

(iv) Narrow-band and short-band SR had similar performances for GBM, LAI, N, and N_C estimation, while both of them had better performances than broad-band TM indices. Hence, the semi-empirical models defined in this study would be exportable to narrow-band (CASI, AISA) or short-band (e.g. AVIRIS, DAIS, HYPERION) airborne or satellite sensors with minimal loss of accuracy.

(v) The main limitations connected with broad-band indices for assessing pasture biophysical properties were related to the reduced number of bands that did not allow identification of the best spectral region for variable estimation, while band width (FWHM) had minor importance.

Acknowledgements

This work was supported by the national project "Sviluppo di Modelli Aziendali Sostenibili e Multifunzionali per la Valorizzazione dei Pascoli in Aree Marginali mediante GIS" (MASO-GIS). The authors gratefully acknowledge L. Busetto, S. Cogliati, A. Marchesi, M. Migliavacca, C. Panigada, M. Rossini (LTDA), A. Monteiro (GeoLab), S. Musinu (NRD), C. Ligios, S. Picconi and A. Pintore (AGRIS) for their support in the experimental setup and in the field work.

References

Asner, G.P., 1998. Biophysical and biochemical sources of variability in canopy reflectance. Remote Sens. Environ. 65, 225–226.
Asner, G.P., Townsend, A.R., Bustamante, M.M.C., 1999. Spectrometry of pasture condition and biogeochemistry in the Central Amazon. Geophys. Res. Lett. 26, 2769–2772.
Asner, G.P., Townsend, A.R., Bustamante, M.M.C., Nardoto, G.B., Olander, L.P., 2004. Pasture degradation in the central Amazon: linking changes in carbon and nutrient cycling with remote sensing. Glob. Change Biol. 10, 844–862.
Bailey, D.W., Gross, J.E., Laca, E.A., Rittenhouse, L.R., Coughenour, M.B., Swift, D.M., Sims, P.L., 1996. Mechanisms that result in large herbivore grazing distribution patterns. J. Range Manage. 49, 386–400.
Ball, D., Collins, M., Lacefield, G., Martin, N., Mertens, D., Olson, K., Putnam, D., Undersander, D., Wolf, M., 2001. Understanding Forage Quality. American Farm Bureau Federation Publication 1-01. American Farm Bureau Federation, Park Ridge, IL.
Beeri, O., Phillips, R., Hendrickson, J., Frank, A.B., Kronberg, S., 2007. Estimating forage quantity and quality using aerial hyperspectral imagery for northern mixed-grass prairie. Remote Sens. Environ. 110, 216–225.
Blackburn, G.A., 1998. Spectral indices for estimating photosynthetic pigment concentrations: a test using senescent tree leaves. Int. J. Remote Sens. 19, 657–675.
Boschetti, M., Bocchi, S., Brivio, P.A., 2007. Assessment of pasture production in the Italian Alps using spectrometric and remote sensing information. Agric. Ecosyst. Environ. 118, 267–272.
Bowyer, P., Danson, F.M., 2004. Sensitivity of spectral reflectance to variation in live fuel moisture content at leaf and canopy level. Remote Sens. Environ. 92, 297–308.
Broge, N.H., Leblanc, E., 2001. Comparing prediction power and stability of broad-band and hyperspectral vegetation indices for estimation of green leaf area index and canopy chlorophyll density. Remote Sens. Environ. 76, 156–172.
Cho, M.A., Skidmore, A., 2006. A new technique for extracting the red edge position from hyperspectral data: the linear extrapolation method. Remote Sens. Environ. 101, 181–193.
Cho, M.A., Skidmore, A., Corsi, F., van Wieren, S.E., Sobhan, I., 2007. Estimation of green grass/herb biomass from airborne hyperspectral imagery using spectral indices and partial least squares regression. Int. J. Appl. Earth Observ. Geoinform. 9, 414–424.
Corrall, A.J., Fenlon, J.S., 1978. A comparative method for describing the seasonal distribution of production from grasses. J. Agric. Sci., UK 91, 61–67.
d'Angelo, M., Enne, G., Madrau, S., Percich, L., Previtali, F., Pulina, G., Zucca, C., 2000. Mitigating land degradation in Mediterranean agro-silvo-pastoral systems: a GIS-based approach. Catena 40, 37–49.
Danson, F.M., Plummer, S.E., 1995. Red-edge response to forest leaf-area index. Int. J. Remote Sens. 16, 183–188.
Darvishzadeh, R., Skidmore, A., Schlerf, M., Atzberger, C., Corsi, F., Cho, M., 2008a. LAI and chlorophyll estimation for a heterogeneous grassland using hyperspectral measurements. ISPRS-J. Photogramm. Remote Sens. 63, 409–426.
Darvishzadeh, R., Skidmore, A., Schlerf, M., Atzberger, C., 2008b. Inversion of a radiative transfer model for estimating vegetation LAI and chlorophyll in a heterogeneous grassland. Remote Sens. Environ. 112, 2592–2604.
Darvishzadeh, R., Skidmore, A., Atzberger, C., van Wieren, S., 2008c. Estimation of vegetation LAI from hyperspectral reflectance data: Effects of soil type and plant architecture. Int. J. Appl. Earth Observ. Geoinform. 10, 358–373.
Daughtry, C.S.T., Walthall, C.L., Kim, M.S., de Colstoun, E.B., McMurtrey, J.E., 2000. Estimating corn leaf chlorophyll concentration from leaf and canopy reflectance. Remote Sens. Environ. 74, 229–239.
Elvidge, C.D., Chen, Z.K., 1995. Comparison of broad-band and narrow-band red and near-infrared vegetation indexes. Remote Sens. Environ. 54, 38–48.
Everitt, J., Richardson, A.J., Gausman, H.V., 1985. Leaf reflectance-nitrogen-chlorophyll relations in buffelgrass. Photogramm. Eng. Remote Sens. 51, 463–466.
FAO/ISRIC/ISSS, 1998. World Reference Base for Soil Resources. World Soil Resources Report 84. FAO, Rome, p. 90.
Feng, W., Yao, X., Zhu, Y., Tian, Y.C., Cao, W., 2008. Monitoring leaf nitrogen status with hyperspectral reflectance in wheat. Eur. J. Agron. 28, 394–404.
Gianelle, D., Guastella, F., 2007. Nadir and off-nadir hyperspectral field data: strengths and limitations in estimating grassland biophysical characteristics. Int. J. Remote Sens. 28, 1547–1560.
Gianelle, D., Vescovo, L., 2007. Determination of green herbage ratio in grasslands using spectral reflectance. Methods and ground measurements. Int. J. Remote Sens. 28, 931–942.
Green, R.N., Trowbridge, R.L., Klinka, K., 1993. Towards a taxonomic classification of humus forms. Forest Sci. 39, 1–49.
Haboudane, D., Miller, J.R., Tremblay, N., Zarco-Tejada, P.J., Dextraze, L., 2002. Integrated narrow-band vegetation indices for prediction of crop chlorophyll content for application to precision agriculture. Remote Sens. Environ. 81, 416–426.

Please cite this article in press as: Fava, F., et al., Identification of hyperspectral vegetation indices for Mediterranean pasture characterization. Int. J. Appl. Earth Observ. Geoinform. (2009), doi:10.1016/j.jag.2009.02.003

Hansen, P.M., Schjoerring, J.K., 2003. Reflectance measurement of canopy biomass and nitrogen status in wheat crops using normalized difference vegetation indices and partial least squares regression. Remote Sens. Environ. 86, 542–553.
He, Y., Guo, X.L., Wilmshurst, J., 2006. Studying mixed grassland ecosystems I: suitable hyperspectral vegetation indices. Can. J. Remote Sens. 32, 98–107.
Hinzman, L.D., Bauer, M.E., Daughtry, C.S.T., 1986. Effects of nitrogen fertilization on growth and reflectance characteristics of winter-wheat. Remote Sens. Environ. 19, 47–61.
Hoffer, R.M., 1978. Biological and physical considerations in applying computer-aided analysis techniques to remote sensor data. In Remote Sensing: The quantitative approach edited by P.H. Swain and S.M. Davis (New York: McGraw-Hill), pp. 227–289.
Hunt, E.R., Everitt, J.H., Ritchie, J.C., Moran, M.S., Booth, D.T., Anderson, G.L., Clark, P.E., Seyfried, M.S., 2003. Applications and research using remote sensing for rangeland management. Photogramm. Eng. Remote Sens. 69, 675–693.
Inoue, Y., Penuelas, J., Miyata, A., Mano, M., 2008. Normalized difference spectral indices for estimating photosynthetic efficiency and capacity at a canopy scale derived from hyperspectral and CO_2 flux measurements in rice. Remote Sens. Environ. 112, 156–172.
Jordan, C.F., 1969. Derivation of leaf area index from quality of light on the forest floor. Ecology 50, 663–666.
Lamb, D.W., Steyn-Ross, M., Schaare, P., Hanna, M.M., Silvester, W., Steyn-Ross, A., 2002. Estimating leaf nitrogen concentration in ryegrass (Lolium spp.) pasture using the chlorophyll red-edge: theoretical modelling and experimental observations. Int. J. Remote Sens. 23, 3619–3648.
Lee, K.S., Cohen, W.B., Kennedy, R.E., Maiersperger, T.K., Gower, S.T., 2004. Hyperspectral versus multispectral data for estimating leaf area index in four different biomes. Remote Sens. Environ. 91, 508–520.
Mutanga, O., Skidmore, A.K., 2004. Narrow band vegetation indices overcome the saturation problem in biomass estimation. Int. J. Remote Sens. 25, 3999–4014.
Mutanga, O., Skidmore, A.K., Prins, H.H.T., 2004. Predicting in situ pasture quality in the Kruger National Park, South Africa, using continuum-removed absorption features. Remote Sens. Environ. 89, 393–408.
Numata, I., Roberts, D.A., Chadwick, O.A., Schimel, J., Sampaio, F.R., Leonidas, F.C., Soares, J.V., 2007. Characterization of pasture biophysical properties and the impact of grazing intensity using remotely sensed data. Remote Sens. Environ. 109, 314–327.
Numata, I., Roberts, D.A., Chadwick, O.A., Schimel, J., Galvao, J., Soares, J.V., 2008. Evaluation of hyperspectral data for pasture estimate in the Brazilian Amazon using field and imaging spectrometers. Remote Sens. Environ. 112, 1569–1583.
Rouse, J.W., Hass, R.H., Shell, J.A., Deering, D.W., 1974. Monitoring vegetation systems in the Great Plains with ERTS-1. In: Proceedings of the 3rd Earth Resources Technology Satellite Symposium 1, 309–317.
Rundquist, B.C., 2002. The influence of canopy green vegetation fraction on spectral measurements over native tallgrass prairie. Remote Sens. Environ. 81, 129–135.
Senft, R.L., Rittenhouse, L.R., Woodmansee, R.G., 1984. Factors influencing patterns of cattle grazing behaviour on shortgrass steppe. J. Range Manage. 38, 82–87.
Starks, P.J., Zhao, D.L., Phillips, W.A., Coleman, S.W., 2006a. Development of canopy reflectance algorithms for real-time prediction of bermudagrass pasture biomass and nutritive values. Crop Sci. 46, 927–934.
Starks, P.J., Zhao, D., Phillips, W.A., Coleman, S.W., 2006b. Herbage mass, nutritive value and canopy spectral reflectance of bermudagrass pastures. Grass Forage Sci. 61, 101–111.
Thenkabail, P.S., Smith, R.B., De Pauw, E., 2000. Hyperspectral vegetation indices and their relationships with agricultural crop characteristics. Remote Sens. Environ. 71, 158–182.
Todd, S.W., Hoffer, R.M., Milchunas, D.G., 1998. Biomass estimation on grazed and ungrazed rangelands using spectral indices. Int. J. Remote Sens. 19, 427–438.
Van Leeuwen, W.J.D., Huete, A.R., 1996. Effects of standing litter on the biophysical interpretation of plant canopies with spectral indices. Remote Sens. Environ. 55, 123–138.
Vescovo, L., Gianelle, D., 2006. Mapping the green herbage ratio of grasslands using both aerial and satellite-derived spectral reflectance. Agric. Ecosyst. Environ. 115, 141–149.
Zarco-Tejada, P.J., Miller, J.R., Noland, T.L., Mohammed, G.H., Sampson, P.H., 2001. Scaling-up and model inversion methods with narrowband optical indices for chlorophyll content estimation in closed forest canopies with hyperspectral data. IEEE Trans. Geosci. Remote Sens. 39, 1491–1507.
Zhao, D.H., Li, J.L., Qi, J.G., 2005. Identification of red and NIR spectral regions and vegetative indices for discrimination of cotton nitrogen stress and growth stage. Comput. Electron. Agric. 48, 155–169.

Please cite this article in press as: Fava, F., et al., Identification of hyperspectral vegetation indices for Mediterranean pasture characterization. Int. J. Appl. Earth Observ. Geoinform. (2009), doi:10.1016/j.jag.2009.02.003